Linearly polarized 'fine structure' of the bright exciton state in individual CdSe nanocrystal quantum dots

H. Htoon,[1] M. Furis,[2] S. A. Crooker,[2] S. Jeong,[1] and V. I. Klimov[1,*]
[1]*Chemistry Division and the Center for Integrated Nanotechnologies, Los Alamos National Laboratory, Los Alamos, New Mexico 87545, USA*
[2]*National High Magnetic Field Laboratory, Los Alamos National Laboratory, Los Alamos, New Mexico 87545, USA*
(Received 2 August 2007; published 22 January 2008)

We report polarization-resolved, low-temperature, high-spectral-resolution studies of the photoluminescence from individual CdSe nanocrystal quantum dots (NQDs). The spectra reveal a 'fine structure' splitting of the bright exciton state in a subset of the studied NQDs. The two fine structure states are spectrally separated by an energy of up to 3 meV depending on NQD size and are characterized by linearly (and orthogonally) polarized emission dipoles. The average splitting scales approximately with inverse NQD volume, consistent with an anisotropic electron-hole exchange interaction which can result from a breakdown of cylindrical symmetry in some of the NQDs.

DOI: 10.1103/PhysRevB.77.035328 PACS number(s): 78.67.Bf, 73.21.La, 73.22.−f, 81.07.Ta

Nanocrystal quantum dots (NQDs) are nanometer-sized crystalline semiconductor particles. Using modern chemical techniques they can be fabricated with nearly atomic precision in a variety of sizes and shapes. As a result of strong quantum confinement, the electronic energies of NQDs are directly dependent on their dimensions. Specifically, by changing NQD size, one can tune the energy gap by hundreds of meV, which translates into wide-range tunability of the emission color.[1] Further, NQDs with well-passivated surfaces show high photoluminescence (PL) quantum yields that approach 100%.[2] All of these properties make colloidal nanocrystals well suited for various light-emitting applications including general lighting, light-emitting diodes,[3] lasers, and optical amplifiers.[4] Recently, the light-emitting properties of NQDs have also been exploited in bio-medical applications[5] that previously mostly utilized organic dyes. Compared to dyes, NQDs offer advantages of higher photochemical stability, reduced emission linewidths, and continuous tunability of emission color throughout the visible and infrared (IR) including the near-IR transparency window of living tissues.[6]

All of these emerging NQD applications require a detailed understanding of both the spectral and polarization properties of NQD emission and, specifically, the structure of the lowest-energy band-edge exciton states. It is well established on both theoretical[7,8] and experimental[9,10] grounds that in spherical (or nearly spherical) colloidal CdSe NQDs, the electron-hole exchange interaction along with the crystal field of the hexagonal lattice split the band-edge exciton (formed from a spin-1/2 electron and spin-3/2 hole) into five energetically distinct states that can be labeled by their angular momentum projection J along the NQD's crystallographic c axis [see Fig. 1(a)]. Of particular importance is the lowest optically active (or "bright") band-edge exciton state, $J=1^L$ (for notation of exciton states in CdSe NQDs, see Refs. 7 and 11). This bright exciton mainly determines the NQD emission properties (the lowest-energy state with $J=2$ is optically forbidden and is typically referred to as a "dark exciton").[11,12] In quantum dots possessing cylindrical symmetry such as prolate particles with major axis along the crystal c axis, this bright exciton is twofold degenerate with regard to the projection of the angular momentum along the c axis (that is, states with projections $|+1\rangle$ and $|-1\rangle$ are nominally degenerate in energy).[13] The corresponding transition dipoles are oriented randomly in the plane normal to the c axis, and emission from such a bright exciton is usually described in terms of a "two-dimensional (2D) planar dipole,"[14] depicted in Fig. 1(a). As observed in previous single-NQD studies, this type of dipole leads to a varying degree of linear PL polarization depending on the orientation of the NQD's c axis with respect to an observation axis.[14,15]

The structure of this emitting bright exciton state changes if the cylindrical symmetry of the quantum dot is broken. In this case, the $J=|\pm 1\rangle$ states become mixed, leading to a fine

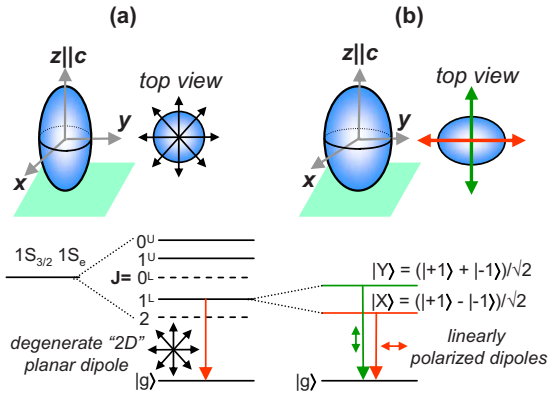

FIG. 1. (Color online) (a) Drawing of a CdSe nanocrystal quantum dot (NQD) having cylindrical symmetry about its crystalline wurtzite c axis and a corresponding structure of electronic states. Exciton states are labeled according to their angular momentum projection J along the c axis. The $|+1\rangle$ and $|-1\rangle$ states comprising the lowest $J=1^L$ "bright" exciton are nominally degenerate in energy. This bright exciton is characterized by a degenerate planar transition dipole oriented isotropically in the plane normal to c. (b) If the NQD's cylindrical symmetry is broken, anisotropic exchange can mix the $|\pm 1\rangle$ states, giving rise to two distinct dipole transitions $|X,Y\rangle$ that emit linearly and orthogonally polarized PL at slightly different energies.

structure splitting of the bright exciton and the associated emission spectra. Symmetry breaking of this type can be expected,[16–18] for example, from slight elongation of the dot along one of its semiminor axes, as depicted in Fig. 1(b). The resulting states, $|X\rangle=(|+1\rangle+|-1\rangle)/\sqrt{2}$ and $|Y\rangle=(|+1\rangle-|-1\rangle)/\sqrt{2}$, are split in energy and are linearly and orthogonally polarized along the nonequivalent semiminor (X and Y) axes of the dot. This type of fine structure has been observed and extensively studied during the past decade in the PL from *epitaxially* grown semiconductor quantum dots.[19–22] High-resolution PL spectra of single epitaxial dots at low temperature clearly show an energy-split doublet that is often linearly polarized along the orthogonal [110] and $[1\bar{1}0]$ axes of the semiconductor substrate (these axes usually determine the direction of the dot's shape distortion). In epitaxial dots, these discrete fine structure exciton states have been cleverly exploited as a basis for quantum entanglement schemes.[23]

In marked contrast, evidence for a fine-structure splitting of bright excitons in colloidal NQDs has only very recently emerged. The polarization-resolved, high spectral resolution PL studies that have been so successfully applied to epitaxially grown quantum dots[19–22] have yet to make a significant impact in colloidal NQD systems. Significantly complicating measurements is the fact that colloidal quantum dots are considerably less photostable than their epitaxially grown counterparts; PL from individual NQDs exhibits blinking, photobleaching, and spectral diffusion as a function of time. These factors render a direct observation of a fine-structure PL doublet more difficult. Furthermore, NQDs are in general oriented randomly in a given sample, such that their crystalline c axes (the axes of cylindrical or near-cylindrical symmetry) point in arbitrary directions with respect to the observation axis. This is quite different than the case of epitaxially grown dots, wherein the growth axis of the sample wafer, which defines *all* the dots' cylindrical or near-cylindrical symmetry axis, can always be oriented along the direction of observation, so that the polarization signatures of the X and Y fine-structure states are easily resolved. The random orientation of NQDs significantly complicates the measured PL polarization properties since X and Y dipoles in a particular NQD may or may not project equally (or at all) on to the observation plane.

The first indications of X-Y fine-structure splitting in NQDs were indirectly inferred from polarization-resolved resonant PL (fluorescence line narrowing) of NQD ensembles in ultrahigh magnetic fields.[24,25] Further indirect evidence was later provided by ultrafast optical four-wave mixing studies of NQD ensembles.[26,27] The first *direct* observation of a polarized X-Y fine-structure splitting in the PL spectra from individual CdSe NQDs was very recently reported by Furis *et al.* in Ref. 25, and a theoretical treatment was subsequently formulated.[28]

Here, we perform low-temperature studies of the emission from individual CdSe NQDs. To mitigate the deleterious effects of blinking and spectral diffusion, we use a high-spectral-resolution imaging microscope to simultaneously monitor both orthogonal, linearly polarized components of the PL from individual NQDs. Using this system, we investigate in detail the spectral and polarization properties of the bright exciton emission. A primary aim of this work is to correlate the PL polarization from a given NQD with its specific three-dimensional orientation in space (not only the orientation of the NQD c axis but also the orientation of the X and Y axes, if resolvable, about the c axis). We measure the polarization properties of hundreds of individual NQDs of varying size and observe that over 40 NQDs exhibit a resolvable fine-structure PL doublet comprised of two linearly and orthogonally polarized peaks. We further observe that the fine structure (X-Y) splitting scales approximately inversely with NQD volume, suggesting that the observed splitting is due to a long-range anisotropic electron-hole exchange interaction. Single-NQD data are in good agreement with the results inferred from earlier, indirect measurements on NQD ensembles.

Figure 2(a) shows a schematic of the experiment. Samples of dilute CdSe/ZnS core/shell NQDs were dispersed in a polymethylmethacrylate matrix onto crystalline quartz substrates (density <0.5 NQD/μm^2). The samples are held at 4 K in a continuous-flow liquid helium cryostat and are excited by 532 nm radiation from a continuous-wave laser that is directed through a microscope objective (numerical aperture of 0.55). Less than 1 mW of laser power is focused to a 20 μm diameter illumination spot on the sample substrate (corresponding average NQD occupancies are less than one electron-hole pair per dot, and hence, the role of multiexciton effects is insignificant). The PL from individual NQDs is collected by the same objective and directed through a polarization rotator (a half-wave plate) and a polarization beamsplitter (a Wollaston prism). This combination spatially separates the emitted PL into orthogonally polarized linear components that are oriented horizontally and vertically with respect to the laboratory reference frame. Both polarization components are then spectrally dispersed in a half-meter imaging spectrometer and are simultaneously detected using spatially distinct regions of a liquid-nitrogen-cooled charge-coupled device (CCD) array. A depolarizer in front of the spectrometer's entrance slit (not shown) ensures the same detection efficiency for both polarization components. The half-wave plate rotates the polarization of the emitted PL with respect to the laboratory reference frame. We extract the NQD orientation and degree of PL linear polarization from a series of spectra taken as the half-wave plate is rotated.

Figure 2(b) shows a typical PL image. Horizontally polarized (HP) and vertically polarized (VP) emissions from individual NQDs are observed as pairs of peaks in the upper and lower regions of the CCD, respectively. Some pairs of peaks (e.g., those connected by dotted arrows) appear at the same energy, indicating no discernible energy difference between HP and VP components. However, many peak pairs (e.g., those indicated by solid arrows) show a clearly resolved energy splitting.

Simultaneous detection of both polarization components demonstrates that these two peaks arise from two distinct emitting states of a *single* NQD, rather than an artifact due to spectral diffusion or due to multiple NQDs. Figure 2(c) shows high-resolution spectra of a particular peak pair (marked by the green arrow). The spectra are derived from line cuts through five spectral images acquired in successive 30 s intervals. Red and black data correspond to VP and HP

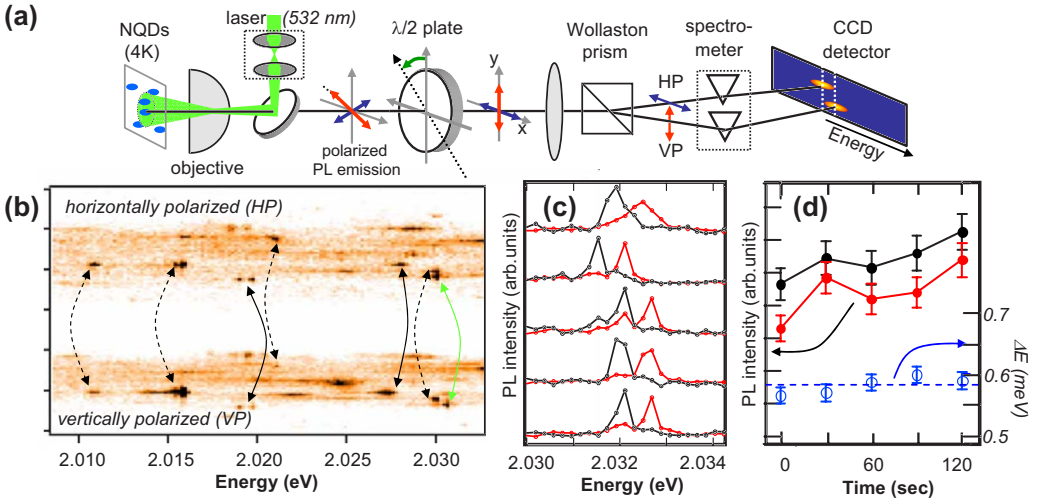

FIG. 2. (Color online) (a) Schematic of the low-temperature, polarization-resolved, single-NQD PL experiment. Both horizontally (HP) and vertically polarized (VP) components from single NQDs are simultaneously acquired on a CCD array, mitigating artifacts due to spectral diffusion and blinking. (b) A typical image showing both HP and VP spectral components from individual NQDs. Some pairs of PL peaks clearly show a fine-structure splitting of 0.2–3.0 meV (e.g., those connected by solid lines). (c) A time series of five spectra from a single NQD (indicated in the image), taken with 30 s intervals. Red and black data points correspond to VP and HP components. (d) The integrated PL of the two polarization components, plotted as a function of time, shows a clear correlation of their intensity fluctuations (left axis). Also shown is the measured fine-structure energy splitting between the peaks, which varies very little (<15 μeV) around an average value of 0.583 meV.

emissions, respectively. The absolute PL intensity, peak position, and line shape of the pair fluctuate as a function of time due to blinking and spectral diffusion effects. Importantly, however, the relative intensities and the energy splitting of the peak pair remain highly correlated, indicating a common emission source. As shown in Fig. 2(d), the two polarization components exhibit correlated intensity fluctuations (red and black points, left axis) and the splitting between the two peaks varies by less than 15 μeV about an average value of 0.58 meV (blue circles, right axis).

Utilizing this detection scheme, we analyze the polarization-resolved PL spectra from hundreds of single NQDs having radii from 1.5 to 4.0 nm (emission energy in the range of 1.95–2.25 eV). Approximately 10% of these NQDs exhibit a resolvable fine-structure splitting. For these NQDs, experimentally measured splittings lie in the range of 0.15–3.0 meV. We do not observe a resolvable splitting between orthogonally polarized PL components in the remainder of the studied NQDs. Reasons for this include (i) the PL emission from some NQDs is spectrally broad, so that a splitting is not resolvable, (ii) some NQDs may not possess any intrinsic bright exciton fine structure, or (iii) the three-dimensional (3D) orientation of the NQD is such that no polarization-resolved splitting is expected.

We now turn to an analysis of the PL polarization properties of individual NQDs, with the goal of determining their full 3D orientation. We begin by showing data from NQDs that *do* show linearly polarized PL, but *do not* exhibit any resolvable fine-structure splitting between its polarized PL components. Figure 3(a) shows spectra from one such NQD, where the five spectra are taken at 40 s intervals and correspond to different orientations of the half-wave plate. Arrows indicate the effective direction of the detected polarization. As observed and discussed above in Fig. 2(c), these polarized PL peaks drift in time due to the effects of spectral diffusion, but otherwise track each other exactly indicating a common source (a single NQD). When the detection axes are set to 20° and 100°, nearly equal amounts of PL are detected in the two orthogonal polarization channels. In contrast, unequal intensities are detected when the effective detection axes are oriented at 0°, 40°, or 120°. Although the intensities of HP and VP emission components oscillate with detection angle, *neither component achieves zero intensity for any detection angle*. As described originally by Empedocles *et al.*,[14] this behavior is a characteristic of a NQD's degenerate 2D "planar" dipole. As depicted in Fig. 3(c), the axis normal to this dipole plane is the c axis of the NQD, which we define here as being tipped by a polar angle θ from the observation axis (z), and rotated about z by an azimuthal angle ϕ_0 with respect to the laboratory reference frame. The projection of the planar dipole onto the observation plane is an elliptical dipole with minor axis oriented along ϕ_0, and with major and minor dimensions having the ratio $1:\cos\theta$ (hence, the linearly polarized PL intensities, proportional to the square of the dipole, have the ratio $1:\cos^2\theta$). For this NQD, Fig. 3(b) shows the normalized HP emission (I_{NH}) as a function of detection angle ϕ [$I_{\mathrm{NH}}=I_{\mathrm{H}}/(I_{\mathrm{H}}+I_{V})$, where $I_{\mathrm{H}/V}$ is the integrated HP/VP emission]. A fit to the data (solid line) reveals that I_{NH} oscillates as $\sin^2(\phi-\phi_0)$ between values of 0.3 and 0.7, indicating that $\theta=49°$ for this NQD. Further, the angle $\phi_0\sim 60°$ for which I_{NH} is minimum indicates the azimuthal orientation of the NQD's c axis with respect to the laboratory reference frame,[14] as schematically shown in Fig. 3(c).

A similar analysis performed on a different NQD is shown in Fig. 3(d). In this case, the PL exhibits a higher degree of linear polarization. As shown in Fig. 3(e), I_{NH} shows $\sin^2(\phi-\phi_0)$ oscillations between values of 0.1 and 0.9, indicating that the projection of this NQD's planar dipole onto

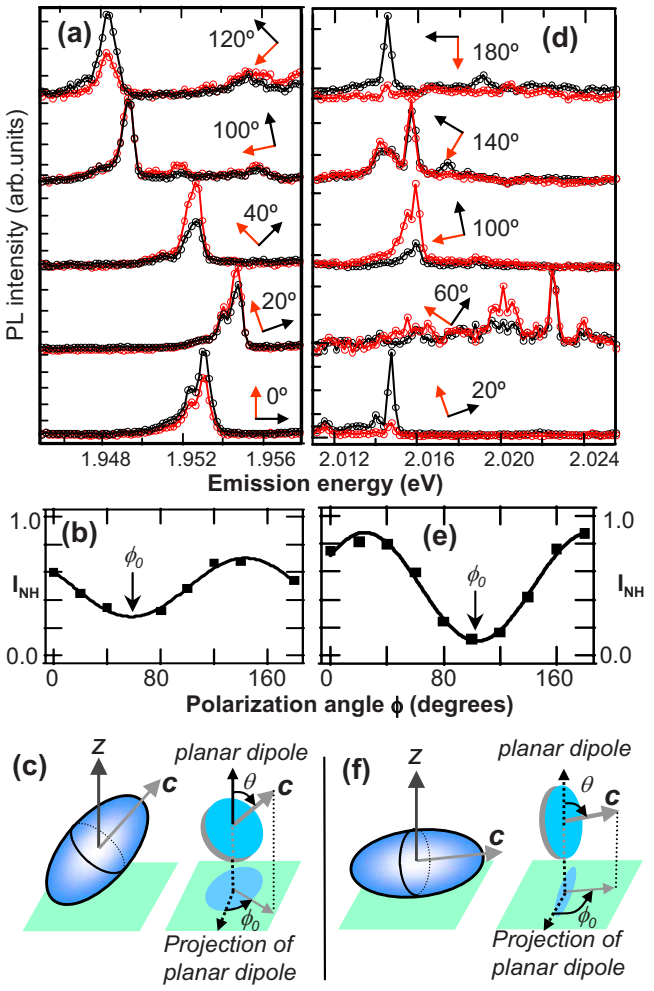

FIG. 3. (Color online) (a) Polarized PL spectra as a function of analyzer (half-wave plate) angle, from a single NQD that emits partially polarized PL, but which does *not* exhibit a resolvable energy splitting between orthogonally polarized PL components. The effective axes of the detected linear polarization are indicated. (b) Data points show the normalized intensity of the horizontal PL component versus detection angle. Line is a sine-squared fit to the data (see text). (c) The 3D orientation of this NQD. [(d)–(f)] Data from a different NQD that exhibits a higher degree of linear polarization (its c axis is nearly perpendicular to the observation axis, as drawn).

the observation plane is a narrow ellipse, as depicted in Fig. 3(f). This NQD is lying almost flat on the substrate with its c axis nearly perpendicular to the observation axis ($\theta=70°$).

A wide variation in the degree of linear polarization from single, randomly oriented CdSe NQDs was first observed in the polarized microscopy studies of Empedocles *et al.*[14] Those studies, which did not spectrally resolve the PL emission, provided the first direct evidence for the 2D planar emission dipole of bright excitons in single NQDs. We now demonstrate that spectrally resolving the polarized PL from single NQDs directly reveals that, in many cases, nominally degenerate 2D planar dipoles actually possess a pronounced X-Y fine structure. Furthermore, the data reveal both the 3D orientation of the NQD's c axis and the orientation of the X and Y fine-structure axes about the c axis.

A resolvable and orthogonally polarized X-Y fine structure splitting was observed in approximately 10% of the studied NQDs, or ~40 in total. Figure 4 shows spectra from three such nanocrystals, each having a different orientation with respect to the observation direction. Figure 4(a) shows polarization-resolved spectra from a single NQD [the same shown in Fig. 2(c)] acquired at five different settings of the half-wave plate. The effective detection axes are indicated by arrows. The two orthogonally polarized PL peaks oscillate nearly out of phase with each other while maintaining their fine-structure energy splitting of 0.58 meV. These data confirm that the two peaks originate from two distinct one-dimensional linear transition dipoles in the same NQD. Figure 4(b) shows the HP emission intensity from both high- and low-energy peaks of the fine-structure doublet. The peaks are highly linearly polarized (>93%), follow a $\cos^2(\phi-\phi_{X,Y})$ intensity dependence, and are orthogonal ($|\phi_X-\phi_Y|=90°\pm1°$). Further, both peaks exhibit nearly equal intensity for all detection orientations—the high- and low-energy peaks account for $48\pm2\%$ and $52\pm2\%$ of the total emission, for all orientations, indicating that both X and Y linear dipoles project equally onto our observation plane. Assuming further that angularly integrated emission intensities produced by the X and Y states are identical,[29] we can conclude that the NQD in this case is oriented with c axis nearly parallel to the observation axis ($c\|z$, $\theta\sim0°$), as schematically depicted in Fig. 4(c), and that the X and Y fine-structure dipoles lie in the observation plane with azimuthal angles ϕ_X and $\phi_Y=20°$ and 110°, respectively.

In the more general (and common) case of a NQD oriented with its c axis at some finite polar angle ($\theta>0°$), X and/or Y fine-structure states no longer both lie within the observation plane defined by z. Thus, their projections onto the observation plane are in general unequal in magnitude, which leads to unequal detected intensities. Figures 4(d)–4(f) illustrate a NQD of this type, where only one of the two fine-structure dipoles projects out of the observation plane. Moreover, if *both* X and Y are tipped out of the observation plane, then their projections onto the observation plane will not necessarily be orthogonal ($|\phi_X-\phi_Y|>90°$). Figures 4(g)–4(i) show a NQD of this latter type.

The second NQD shown in Figs. 4(d)–4(f) exhibits an X-Y fine-structure splitting of 1.1 meV. Like the previous NQD shown in panel (a), the two peaks are highly linearly polarized (>86%) and are nearly orthogonal ($|\phi_X-\phi_Y|=90°\pm1°$). However, the intensity of the high-energy peak is much weaker, contributing only ~35% of the total PL emission at all detection angles. Based on these data and further assuming that X and Y states equally contribute to PL,[29] we obtain that the low-energy dipole lies nearly in the observation plane (with $\phi_X\sim150°$), while the higher-energy dipole is tipped out of the observation plane by the polar angle $\theta=25°$, as depicted in Fig. 4(f).

In the third case, the NQD shown in Figs. 4(g)–4(i) exhibits X and Y emission peaks with linear polarization >75% (the lower polarization in this case results from the broad tail of the PL peaks). However, the two peaks exhibit significantly different intensities ($76\pm4\%$ vs $24\pm4\%$), and their polarization orientations are not orthogonal ($|\phi_X-\phi_Y|$

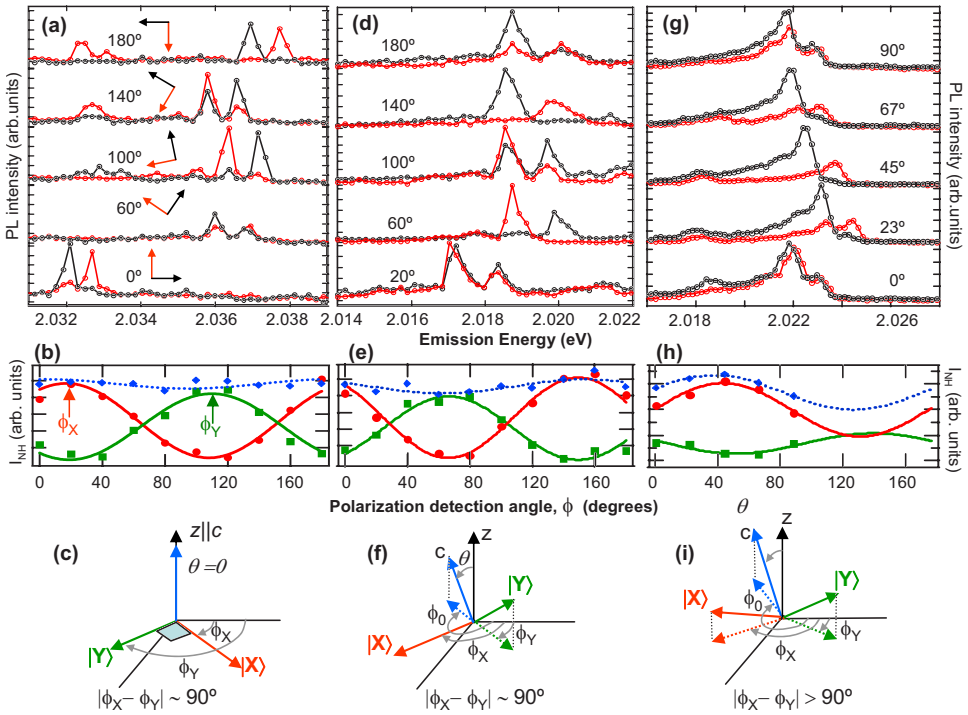

FIG. 4. (Color online) The upper panels [(a), (d), and (g)] show polarized PL spectra from three different NQDs that *do* exhibit a fine-structure splitting between orthogonally polarized PL components. The effective detection angles are indicated in the spectra. The middle panels [(b), (e), (h)] show the angle-dependent intensities of the HP component of the high-energy peak (green points) and low-energy peak (red points), normalized to total PL intensity. Lines are fits to the data. The lower panels [(d), (f), and (i)] depict the inferred orientation of the *c*, *X*, and *Y* axes of these three NQDs.

~100°). These data are indicative of a NQD oriented with both *X* and *Y* transition dipoles oriented out of the observation plane, as depicted in Fig. 4(i).

Spectrally resolving the polarized PL from single NQDs is required to observe the fine-structure splitting of the bright exciton. However, we note that spectrally *integrating* the HP or VP emission recovers the angle-dependent intensity oscillations [blue points in Figs. 4(b), 4(e), and 4(h)] observed in prior work[14,15] which was polarization-resolved but not spectrally resolved. Analyzing only the PL polarization, as in Refs. 14 and 15, provides correct results for the *c*-axis orientation regardless of whether the bright exciton exhibits an *X*-*Y* fine-structure splitting or not. All these observations are, of course, predicated on the assumption that *X* and *Y* states equally contribute to PL.[29]

Finally, we examine the dependence of the fine-structure splitting observed for 40 NQDs on their inverse volume $1/V$ (Fig. 5).[30] The energy splitting shows significant variations (from 0.5 to 3.0 meV), indicating a wide variation in the degree of shape anisotropy in CdSe NQDs studied in this work. Despite this wide variation, the data also exhibit an overall trend of gradual increase in the splitting with $1/V$. To analyze this trend in more quantitative terms, we divide the data points into bins [indicated in Fig. 5(a) by the dashed lines] and calculate the average values of both $1/V$ and the energy splitting for each bin. These data (open circles) are plotted in Fig. 5(b) together with the results of our earlier high-magnetic-field experiments from NQD ensembles[25] (solid dots). We observe a clear correspondence between these two data sets. A clear $1/V$ scaling is apparent in both sets of data and is in agreement with theories[16–18,28] that ascribe the *X*-*Y* splitting to the long-range, anisotropic electron-hole exchange interaction.

In principle, in addition to lateral shape asymmetry, the *X*-*Y* splitting in quantum dots can also be contributed by strain-induced piezoelectric fields. These two contributions are characterized by distinctly different size dependences. The splitting due to shape asymmetry increases with decreasing quantum dot size, while the splitting due to the piezoelectric effect shows an opposite trend. Depending on the exact composition of the dot and/or matrix both of these trends have been observed experimentally for epitaxial quantum dots.[31,32] Furthermore, in the case when the *X*-*Y* splitting is dominated by the piezoelectric effect, the value of the

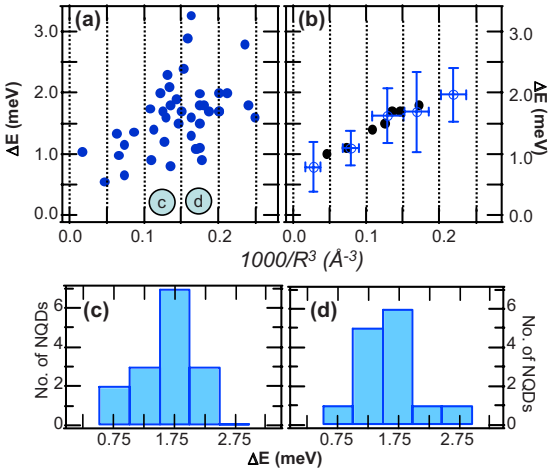

FIG. 5. (Color online) (a) The measured *X*-*Y* fine-structure splitting in 40 individual NQDs, plotted as a function of the estimated inverse NQD volume. These data are binned by inverse volume (dotted lines), and the open circles and error bars in (b) show the mean and standard deviation within each bin. These points overlap well with the solid points, which represent the ensemble-averaged fine-structure splitting derived from fluorescence-line-narrowing studies of NQD ensembles in high magnetic fields (from Ref. 25): (c) and (d) show statistics of the measured fine structure splitting in the third and fourth bins from panel (a), respectively.

piezoelectric constant derived from experimental data is distinctly different (even signwise) from that of a parental bulk solid. This discrepancy suggests strong influence of strains that develop at quantum-dot/matrix interfaces. The effect of strains is less important in colloidal nanocrystals that represent freestanding particles. Hence, in this case, the *X*-*Y* splitting is expected to be primarily due to shape anisotropy. This conjecture is supported by the $1/V$ scaling indicated by experimental data in Fig. 5.

It is also notable that while the values of the fine-structure splitting reported for epitaxial quantum dots are typically from a few hundred μeV (Refs. 19–23) to 1.0 meV,[33] the splitting observed here for colloidal nanocrystals can be as large as 3.2 meV. One likely reason for this difference is the significant volume difference between colloidal and epitaxial quantum dots. While the latter can have small heights of only a few nanometers, they are usually characterized by larger lateral dimensions ($>$10 nm). As a result, the volume of epitaxial dots typically exceeds that of colloidal nanocrystals and leads to (according to the $1/V$ scaling) a smaller *X*-*Y* splitting.

In conclusion, these polarization-resolved and high-spectral resolution studies of individual NQDs provide direct evidence that the bright exciton, which is often regarded to have a degenerate planar transition dipole, can actually possess an *X*-*Y* fine structure consisting of two linearly (and orthogonally) polarized states. In analogy with epitaxial quantum dots, this fine-structure splitting likely results from breaking the NQD cylindrical symmetry. While the magnitude of the fine-structure splitting measured in these colloidal nanocrystals is larger than those typically observed in epitaxial dots, further theoretical studies are essential to quantitatively understand this effect and to extend currently existing models of NQD band-edge exciton fine structure.

This work was supported by the Chemical Sciences, Biosciences and Geosciences Division of the Office of Basic Energy Sciences, U.S. Department of Energy (DOE), Los Alamos LDRD funds, and the Center for Integrated Nanotechnologies jointly operated for DOE by Los Alamos and Sandia National Laboratories. We thank Anna Trugman for her assistance in data extraction.

*klimov@lanl.gov

[1] A. P. Alivisatos, Science **271**, 993 (1996).
[2] L. Qu and X. Peng, J. Am. Chem. Soc. **124**, 2049 (2002).
[3] V. L. Colvin, M. C. Schlamp, and A. P. Alivisatos, Nature (London) **370**, 354 (1994).
[4] V. I. Klimov, A. A. Mikhailovsky, S. Xu, A. Malko, J. A. Hollingsworth, C. A. Leatherdale, H. J. Eisler, and M. G. Bawendi, Science **290**, 314 (2000).
[5] W. J. Parak, D. Gerion, T. Pellegrino, D. Zanchet, C. Micheel, S. C. Williams, R. Boudreau, M. A. Le Gros, C. A. Larabell, and A. P. Alivisatos, Nanotechnology **14**, R15 (2003).
[6] S. Kim, Y. T. Lim, E. G. Soltesz, A. M. De Grand, J. Lee, A. Nakayama, J. A. Parker, T. Mihaljevic, R. G. Laurence, D. M. Dor, L. H. Cohn, M. G. Bawendi, and J. V. Frangioni, Nat. Biotechnol. **22**, 93 (2004).
[7] Al. L. Efros, in *Semiconductors and Metal Nanocrystals*, edited by V. I. Klimov (Dekker, New York, 2004).
[8] M. Chamarro, C. Gourdon, P. Lavallard, O. Lublinskaya, and A. I. Ekimov, Phys. Rev. B **53**, 1336 (1996).
[9] D. J. Norris, Al. L. Efros, M. Rosen, and M. G. Bawendi, Phys. Rev. B **53**, 16347 (1996).
[10] U. Woggon, F. Gindele, O. Wind, and C. Klingshirn, Phys. Rev. B **54**, 1506 (1996).
[11] M. Nirmal, D. J. Norris, M. Kuno, M. G. Bawendi, Al. L. Efros, and M. Rosen, Phys. Rev. Lett. **75**, 3728 (1995).
[12] S. A. Crooker, T. Barrick, J. A. Hollingsworth, and V. I. Klimov, Appl. Phys. Lett. **82**, 2793 (2003).
[13] Note, however, that a small splitting can arise from crystal structure alone, as described, for example, in A. Franceschetti, L. Wang, H. Fu, and A. Zunger, Phys. Rev. B **58**, R13367 (1998).
[14] S. A. Empedocles, R. Neuhauser, and M. G. Bawendi, Nature (London) **399**, 126 (1999).
[15] I. H. Chung, K. T. Shimizu, and M. G. Bawendi, Proc. Natl. Acad. Sci. U.S.A. **100**, 405 (2003).
[16] E. L. Ivchenko, Phys. Status Solidi A **164**, 487 (1997).
[17] S. V. Gupalov, E. L. Ivchenko, and A. V. Kavokin, JETP **86**, 388 (1998).
[18] T. Takagahara, Phys. Rev. B **62**, 16840 (2000).
[19] M. Bayer, A. Kuther, A. Forchel, A. Gorbunov, V. B. Timofeev, F. Schafer, J. P. Reithmaier, T. L. Reinecke, and S. N. Walck, Phys. Rev. Lett. **82**, 1748 (1999).
[20] D. Gammon, E. S. Snow, B. V. Shanabrook, D. S. Katzer, and D. Park, Phys. Rev. Lett. **76**, 3005 (1996).
[21] V. D. Kulakovskii, G. Bacher, R. Weigand, T. Kummell, A. Forchel, E. Borovitskaya, K. Leonardi, and D. Hommel, Phys. Rev. Lett. **82**, 1780 (1999).
[22] J. Puls, M. Rabe, H.-J. Wunsche, and F. Henneberger, Phys. Rev. B **60**, R16303 (1999).
[23] N. H. Bonadeo, J. Erland, D. Gammon, D. Park, D. S. Katzer, and D. G. Steel, Science **282**, 1473 (1998).
[24] M. Furis, T. Barrick, P. Robbins, S. A. Crooker, M. A. Petruska, V. I. Klimov, and Al. L. Efros, Int. J. Mod. Phys. B **18**, 3769 (2004).
[25] M. Furis, H. Htoon, M. A. Petruska, V. I. Klimov, T. Barrick, and S. A. Crooker, Phys. Rev. B **73**, 241313(R) (2006).
[26] A. I. Filin, P. D. Persans, K. Babocsi, M. Schmitt, W. Kiefer, V. D. Kulakovskii, and N. A. Gippius, Phys. Rev. B **73**, 125322 (2006).
[27] G. D. Scholes, J. Kim, C. Y. Wong, V. M. Huxter, P. S. Nair, K. P. Fritz, and S. Kumar, Nano Lett. **6**, 1765 (2006).
[28] S. V. Goupalov, Phys. Rev. B **74**, 113305 (2006).
[29] A notion that the *X* and the *Y* states contribute equally to the angularly integrated PL is based on the assumption that the product of the transition oscillator strength and the occupation factor is not significantly different between these two states. The latter situation can be realized, for example, if an increase in the *X*-*Y* energy splitting is accompanied by simultaneous growth in the oscillator strength of the higher-energy state. While we have some experimental evidence that this behavior is indeed observed in CdSe NQDs, we still would like to emphasize that

until it is rigorously proven that the contributions of the *X* and *Y* states into the overall emission intensity are identical, the results of the analysis of the 3D orientation of NQDs conducted in this paper should be considered as tentative.

[30] The size of the individual NQDs was inferred from the measured PL emission energy and was corroborated by the size-dependent bright-dark splitting that we measured separately in low-temperature fluorescence line narrowing studies of size-selected NQD ensembles.

[31] M. Bayer, G. Ortner, O. Stern, A. Kuther, A. A. Gorbunov, A. Forchel, P. Hawrylak, S. Fafard, K. Hinzer, T. L. Reinecke, S. N. Walck, J. P. Reithmaier, F. Klopf, and F. Schafer, Phys. Rev. B **65**, 195315 (2002).

[32] R. Seguin, A. Schliwa, S. Rodt, K. Potschke, U. W. Pohl, and D. Bimberg, Phys. Rev. Lett. **95**, 257402 (2005).

[33] V. Türck, S. Rodt, R. Heitz, O. Stier, M. Strassburg, U. W. Pohl, and D. Bimberg, Phys. Status Solidi B **224**, 217 (2001).